JOURNAL OF MATERIALS SCIENCE 24 (1989) 2957–2966

Shear cutting of PET film

D. BOLLEN, J. DENEIR, E. AERNOUDT
Department of Metallurgy and Materials Engineering, Catholic University of Leuven, B3030 Heverlee, Belgium

W. MUYLLE
Agfa-Gevaert N.V., B2510 Mortsel, Belgium

Poly(ethylene terephthalate) (PET) film was extruded and then successively biaxially stretched and thermofixed to obtain a high-strength film with stable dimensions. Next, the film was shear cut by two rotating circular knives. In the first part of this paper, a microscopic evaluation of the sheared edges of films, cut under a variety of parameters, i.e. cutting speed, film thickness and knife angle, is given. A particular cutting defect, namely the formation of fibres, is discussed. In the second part, a theory for the shear cutting process of PET film and the related fibre formation is presented. Special attention is paid to the influence of the film manufacturing parameters (applied in this study) on the behaviour of the material during shear cutting.

1. Introduction

High-strength PET can be obtained in combination with good chemical, thermal and several other interesting properties at a relatively low cost. For this reason, it is frequently selected as material for bottles, films and fibres. Many other applications have also been reported [1].

The present paper deals with phenomena occurring during the shear cutting of polymer films in general and PET film in particular. Specific to PET, the possible formation of fibres is a problem. They deteriorate the optical and mechanical quality of, for example, a camera. When dispersed over the photosensitive emulsion, they give rise to the well-known scattering stripes on the screen. Fibre formation depends on the cutting parameters, but also on the PET microstructure, which can be influenced by the previous processing parameters.

2. Experimental details

2.1. Material

Semi-crystalline PET film has been provided by the laboratories of Agfa-Gevaert, Belgium. The manufacturing of the film samples consisted of three steps. Initially, melted PET was extruded through a rectangular slit and quenched by contact with water-cooled rollers. The cooling rate was high enough to obtain an amorphous film. Secondly, the film was biaxially stretched in two steps. In the first step a longitudinal stretching ratio of about 3.5 was given. The crystallinity index (measured by density variation) increased during this process to 30% (volume per cent). In the second step the film was stretched in the transverse direction with a stretching ratio of 3.3, in which the degree of crystallinity decreased to 25%. Finally, the film was thermofixed at a temperature above 200° C. This process increased the degree of crystallinity to 50%. Films of different thicknesses were made, ranging between 63 and 120 μm.

2.2. Cutting geometry and working conditions

The film was shear cut in longitudinal direction by two rotating circular knives (Fig. 1). The lower knife has a cylindrical shape and carries the film during the cutting process. The upper knife has a dish-like shape. The two knives have a minimum overlap distance to avoid damage while rotating [2]. Overlap distance and knife diameters determine the cutting angle (Figs 1 and 2). Continuous but elastic contact between the knives was realized with a compressive spring mounted on the upper knife axis: a clearance [3] between the upper and lower knives must be avoided [2], to prevent the highly compressible PET film from being pinched between the knives instead of being cut by them. A rounding off at the right part of the lower knife, called the shoulder, avoids damage to the film caused by folding. The upper knife is characterized by a knife angle at its tip (Fig. 3). It rotates at a higher peripheral velocity than the lower one, to obtain a relatively vertical penetration into the film (Fig. 1) [2].

The two edges [3] of the cut film are called by definition its front face and its back face, the former one resting on the lower knife, the latter being in contact with the upper knife (Fig. 3).

Several cutting speeds were used corresponding with initial compressive strain rates (ICSR) of 117 to 4432 sec^{-1}. The initial compressive strain rate (an idealized but significant strain rate in the thickness direction) is determined at the instant and place where the upper knife makes contact with the film surface (point A, Fig. 2) and can easily be derived from the cutting angle (α), the film thickness (d) and the peripheral velocity of the lower knife (v_1) (Figs 1 and 2)

0022–2461/89 $03.00 + .12

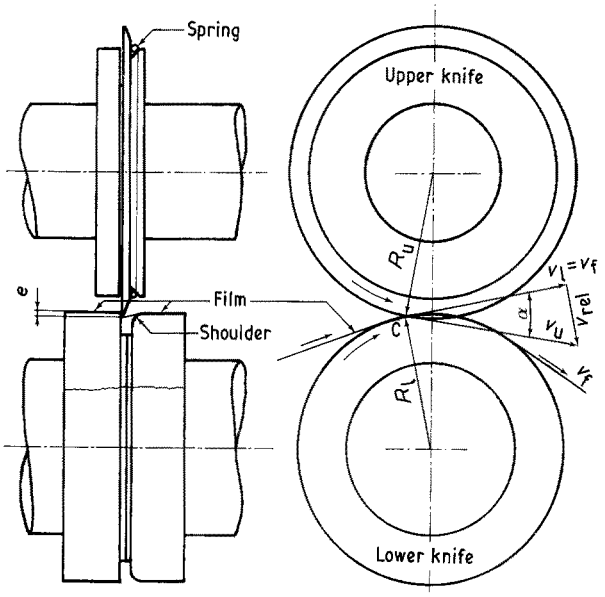

Figure 1 Set up for the shear cutting of PET-film. R_u and R_l are the diameters of upper and lower knife, respectively; v_u and v_l are the respective peripheral velocities at the intersection of the knife edges (point C), and v_{rel} is the relative velocity of the upper knife; v_f is the film velocity, α is the cutting angle and e is the overlap distance.

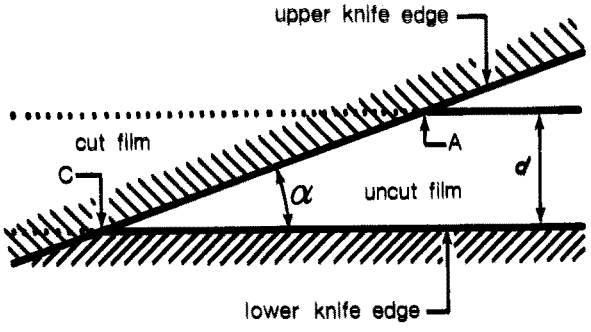

Figure 2 Detailed schematic view at point C of Fig. 1; d is the film thickness.

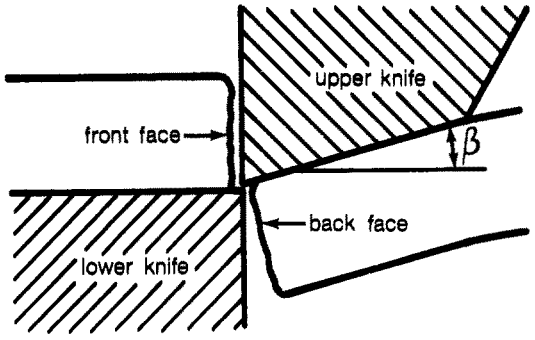

Figure 3 View of a section (between points A and C of Fig. 2, and perpendicular to the lower knife edge), with definitions of front face, back face and upper knife angle (β).

$$\text{ICSR} = [v_l \tan(\alpha)]/d \qquad (1)$$

The initial compressive strain rate is also equal to the initial shear strain rate, if the width of the sheared zone (in transverse direction) is assumed to be equal to the film thickness (d).

3. Results

3.1. Description of the sheared edges

Samples have been investigated using a scanning electron microscope ISI-SS60. Four different regions can be distinguished on the sheared edges (Fig. 4): the scales region, the split region and the upper and lower flaps regions. They appear at the front face as well as at the back face and their dimensions vary with changing cutting parameters. Sometimes some of these regions do not form at all. The dependence of the size of the regions on cutting speed and film thickness, as measured by experiments, is schematically shown in Fig. 5 (front and back face of a 63 μm thick film).

3.1.1. Description of the scales region

Scales form only in the upper part of the front face and in the lower part of the back face (Fig. 4). They are vertical or almost vertical and start at the top (front face) or the bottom (back face). At low cutting speed, the scales are very long and cover most of the edge (Fig. 6). At high speed, they are short and sometimes only visible at great magnification (Fig. 7). A linear relationship can be found between the scale length to film thickness ratio (relative scale length in percent) and the logarithm of the initial compressive strain rate (Fig. 8). The influence of film thickness and the difference between front face and back face (see also Fig. 5) are of secondary importance.

The relative scale density (scale length to interscale distance ratio) decreases with the cutting speed. At high cutting speed, fewer scales are present and they mostly appear separately. At low speed, the whole edge is covered by scales. At the lowest speed, a scale is usually partly overlapped by the scale formed next to it (lying to the right of it at the front face, and to the left of it at the back face, as is indicated by the arrows in Fig. 4).

At either side of a scale horizontal ribs can be seen (Fig. 6). Compared to the scales, they are small, except the ribs at the right side of the front face scales at higher cutting speeds (Fig. 7).

3.1.2. Description of the split region

This region is situated at the bottom of the front face and at the top of the back face (Fig. 4). The material seems to be horizontally cleft (Fig. 9). The height of that region also decreases with cutting speed but is difficult to measure. Indeed, the region interferes with the scales at lower speeds, while at higher speeds it is quite small.

3.1.3. Description of the upper and lower flaps regions

The upper flaps region appears below the scales at the front face and below the split region at the back face (Fig. 4). It has a flat surface, although at high magnification it shows a rugged, laminated structure (Fig. 7). This region is characterized by several flaps, hanging out of the edge (Fig. 10), which were drawn out of the opposite edge, where the corresponding voids can be seen. However, flaps are mostly bent over the edge (and even back fastened) and cover the underlying surface and voids. At the front face, they are bent downwards, and at the back face upwards, but less so than at the front face. The flaps are not horizontal but have a slope: positive at the front face and negative at the back face (Fig. 4).

Finally, the lower flaps region is situated under the

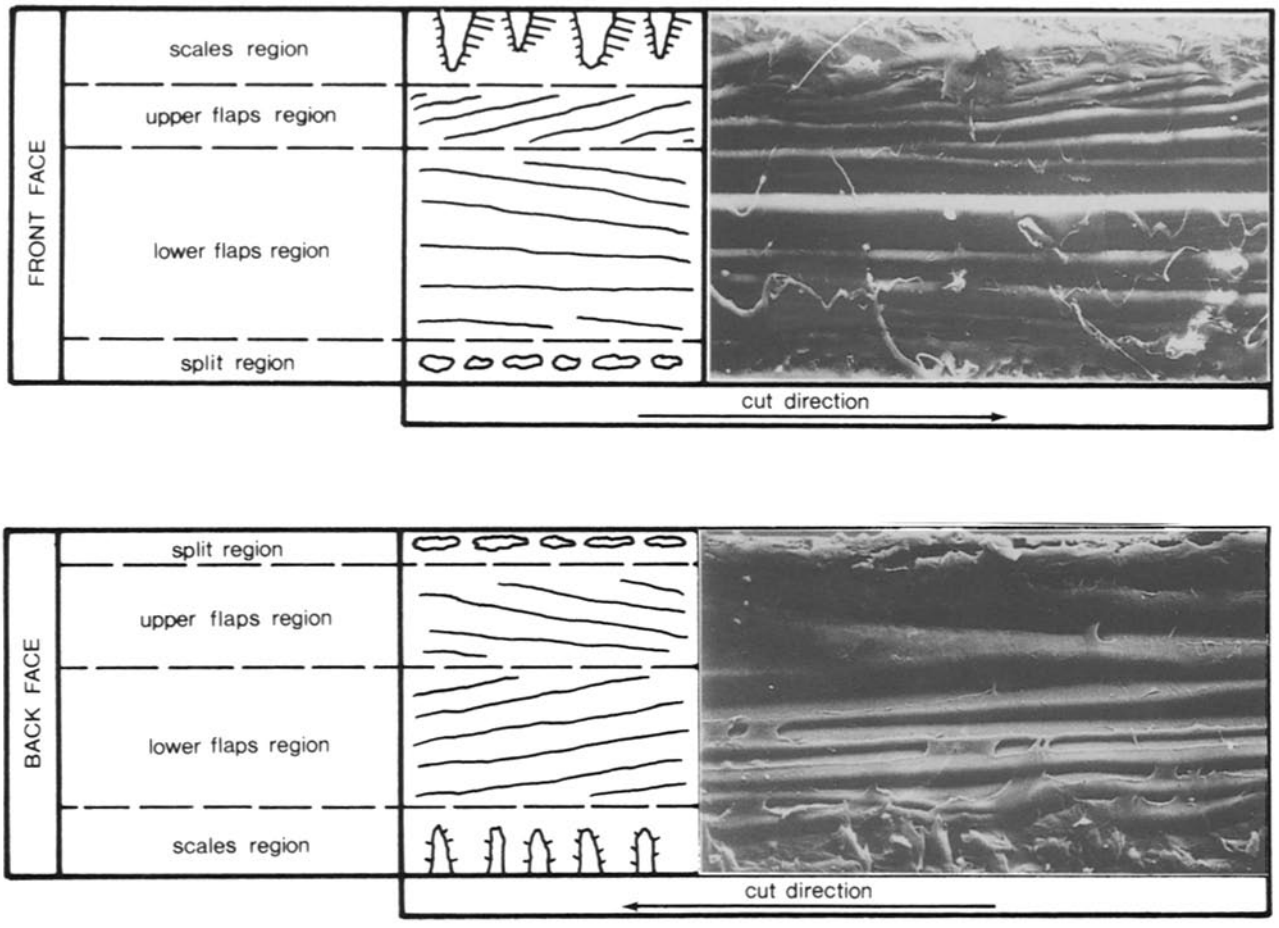

Figure 4 Definitions of the different regions, appearing at the cut edges. The arrows indicate the direction in which the film has been cut. Front face photograph: $d = 130\,\mu m$, ICSR $= 1289\,sec^{-1}$; back face photograph: $d = 63\,\mu m$; ICSR $= 3544\,sec^{-1}$).

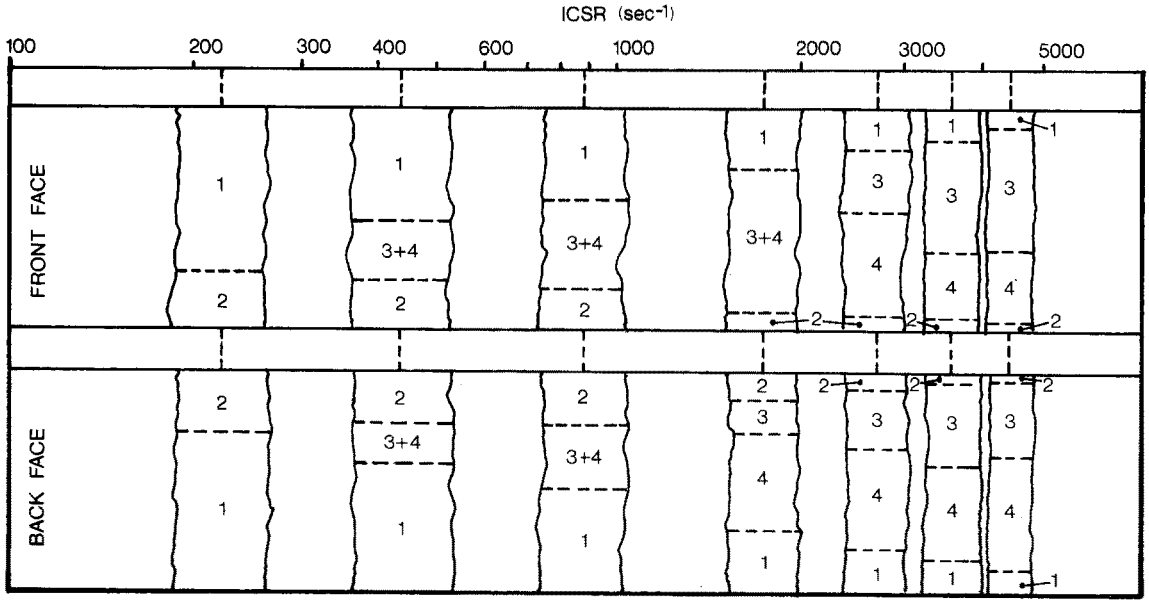

Figure 5 Influence of the initial compressive strain rate (ICSR) on the appearance of the different regions on the cut edges ($d = 63\,\mu m$). The numbers 1, 2, 3 and 4 refer to the scales region, the split region and the upper and lower flaps regions, respectively.

upper flaps region (Fig. 4). It is almost identical to the upper flaps region, but the flaps have an opposite slope, i.e. a negative one at the front face and a positive one at the back face. However, the slope is less steep: the flaps are almost horizontal.

Because the scales region and the split region are smaller at high cutting speeds, the size of the flaps regions increases with speed. At low speeds, upper and lower flaps cannot be distinguished from each other because only a few flaps exist. At the lowest speeds, they disappear because the whole surface is covered by the scales and the split region.

3.2. Description of the cutting defects

After a film has been cut, horizontal fibres, typical of this kind of film, can sometimes be seen. Three kinds

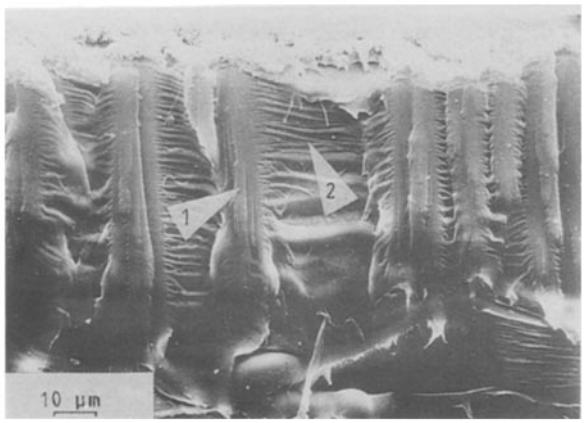

Figure 6 View of the upper part of a front face (d = 130 μm), at low cutting speed (ICSR = 117 sec^{-1}): (formation of long scales (arrow 1) and horizontal ribs (arrow 2).

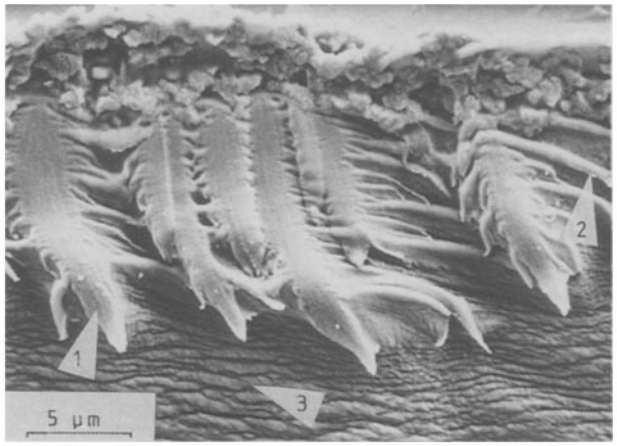

Figure 7 View of the upper part of a front face (d = 100 μm), at high cutting speed (ICSR = 2650 sec^{-1}): formation of short scales (arrow 1) and relatively large ribs (arrow 2). Arrow 3 indicates the laminated structure in the upper flaps region.

of fibre can be observed at the sheared edges: top fibre, central fibre and bottom fibre. Their names are related to the place where they form; sometimes they are displaced from that position in subsequent phases of the cutting process.

The top fibre is formed at the upper layer of the

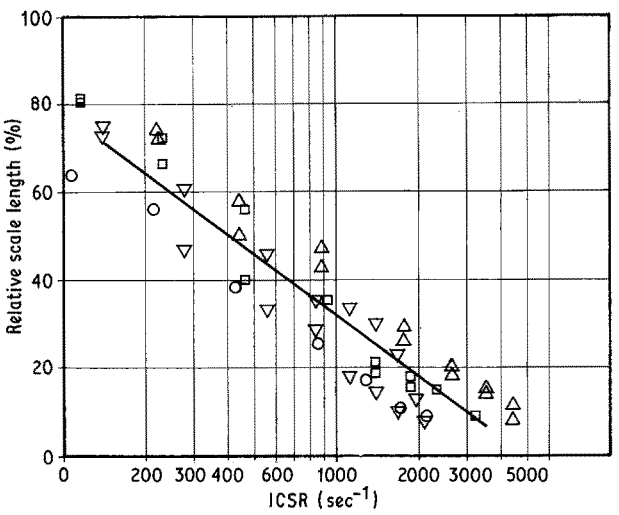

Figure 8 Relationship between the relative scale length and the initial compressive strain rate (ICSR). Film thickness: (△) 63 μm, (▽) 100 μm, (□) 120 μm, (○) 130 μm.

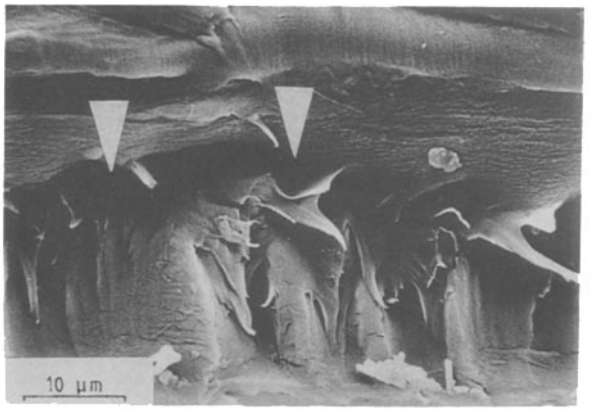

Figure 9 View of the lower part of a front face (d = 120 μm, ICSR = 465 sec^{-1}): the arrows show the split region.

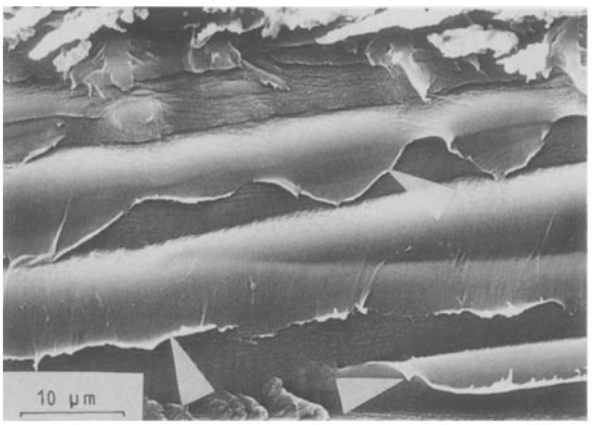

Figure 10 View of the upper flaps zone of a front face (d = 100 μm, ICSR = 2094 sec^{-1}): the arrows indicate the flaps, which were pulled out of the opposite edge.

front face and/or the back face of the film (Fig. 11). It has a ribbon-like form. With small knife angles, less than about 10°, the fibre only forms at the front face, with wide knife angles (more than about 10°), only at the back face. Using an intermediate angle causes fibres to form at both faces, but less frequently than in the other cases. Finally, the formation of fibres (i.e. length and/or thickness of the fibres, and/or total fibre length per unit length of the cut) decreases at higher speeds and with thinner films.

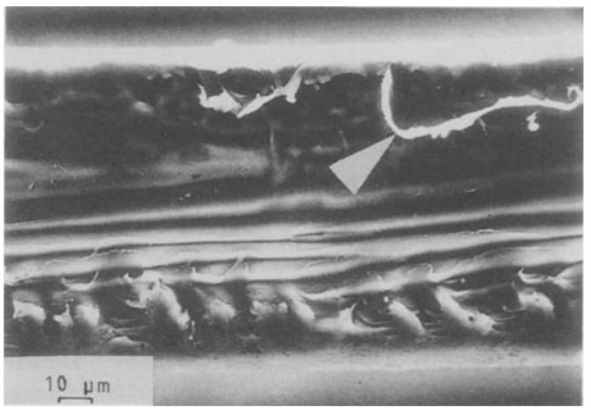

Figure 11 Formation of a top fibre (arrow) at the back face (d = 120 μm, ICSR = 1396 sec^{-1}).

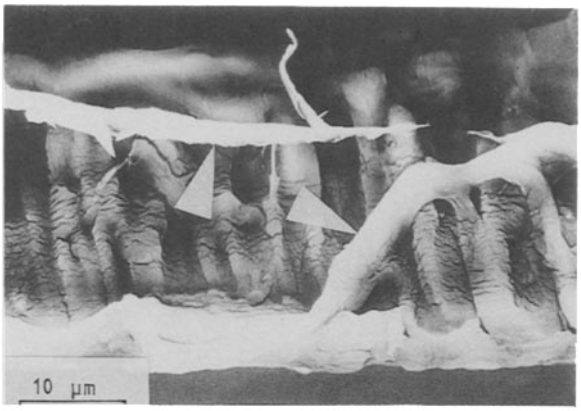

Figure 12 Formation of a bottom fibre (arrows) at the front face (d = 100 µm, ICSR = 838 sec^{-1}).

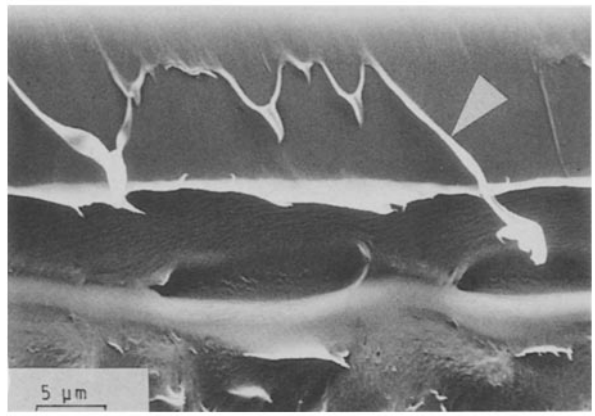

Figure 13 Formation of a central fibre (arrow) at the front face (d = 100 µm, ICSR = 838 sec^{-1}).

The bottom fibre is always formed and observed in the lower part of the front face (Fig. 12) and is much thicker than the top fibre. The dependence of its formation on the cutting parameters is less obvious. However, a blunt lower knife enhances its formation, as do lower cutting speeds and thicker films.

Finally, the central fibre is formed somewhere in the middle of the edge, mostly at the lower flaps region of the front face (Fig. 13). It only exists at higher cutting speeds and is very thin.

4. Discussion

4.1. Microstructure of biaxially stretched and thermofixed film

As the microstructure influences the cutting behaviour of the material, it is necessary to consider the influence of the preceding production steps of PET film on its microstructure.

4.1.1. Microstructure after extrusion

Molten PET material was extruded through a rectangular slit and quenched. Although an amorphous film was obtained, ordering on a molecular scale occurred. During extrusion, chains were oriented along the extrusion direction [4]. However, as the temperature was high before cooling, chains were randomly reoriented. X-ray diffraction patterns show a non-oriented crystalline phase (crystallisation from the melt with a crystallinity index of 1%). The impact of ordering during cutting is negligible, because the microstructure drastically changes in the subsequent steps.

4.1.2. Microstructure after longitudinal stretching

The stretching conditions (i.e. sufficiently high drawing ratio and rate in relation to drawing temperature [5]), enable polymer chains to be oriented along the drawing axis. Because stretching is executed above the glass transition temperature (70° C), strain-induced crystallization to a degree of about 30% was measured. The amorphous phase is also mainly oriented.

The oriented crystals are probably of the "shish-kebab" type [4, 6] (Fig. 14c [6]), which contain extended polymer chains (nuclei), where lamellar crystals have grown with their chains parallel to the nucleus. The crystallites (see Fig. 15 [7] for the unit cell) exhibit a uniplanar-axial orientation, where the c-axis orients parallel to the drawing direction and the (1 0 0) plane parallel to the film surface [8]. The latter characteristic originates from stretching under an almost constant width (by appropriate boundary conditions), which involves plane strain deformation (a thickness reduction of nearly the drawing ratio).

Reflecting this macroscopic behaviour, the section of the separate extended crystal superstructures is assumed to be not round, but elliptical. This suggests that there is a laminated film structure (preferentially parallel to the surface), rather than a fibrillar structure (i.e. round fibrils). Laminated structures are still enhanced by eventual flow and temperature gradients in the perpendicular direction during drawing, especially at the surfaces (symmetry consideration).

4.1.3. Microstructure after transverse stretching

The transverse stretching was also executed above the glass transition temperature, making transverse strain-induced crystallization possible (also into shish-kebab structures). However, there is a considerable difference between transverse and longitudinal stretching, because the "basic" materials are very different.

During transverse stretching, the structure of the longitudinal crystals is, at least partially, destroyed [9]. They can exhibit amorphous ordering in the longitudinal direction, or they can be partially rearranged into an amorphous phase (completely amorphous, or oriented in the transverse direction), or wound off to form transverse crystals [10]. The remaining amorphous phase (after longitudinal stretching) is partially transformed into completely amorphous phase, or into transversely oriented amorphous phase, or into transversely oriented crystals. Thus, by the damaging effect of transverse stretching on longitudinal crystals, and conversely the hindering effect of their presence on the formation of transverse crystals, the total degree of crystallinity decreases from 30% to 25% [11]. The degree of uniplanar orientation increases, and the c-axes orient preferentially in longitudinal or transverse direction [8].

The laminated character of the film is enhanced by the transverse stretching. The longitudinal ribbon-like superstructures become nearly parallel to the film

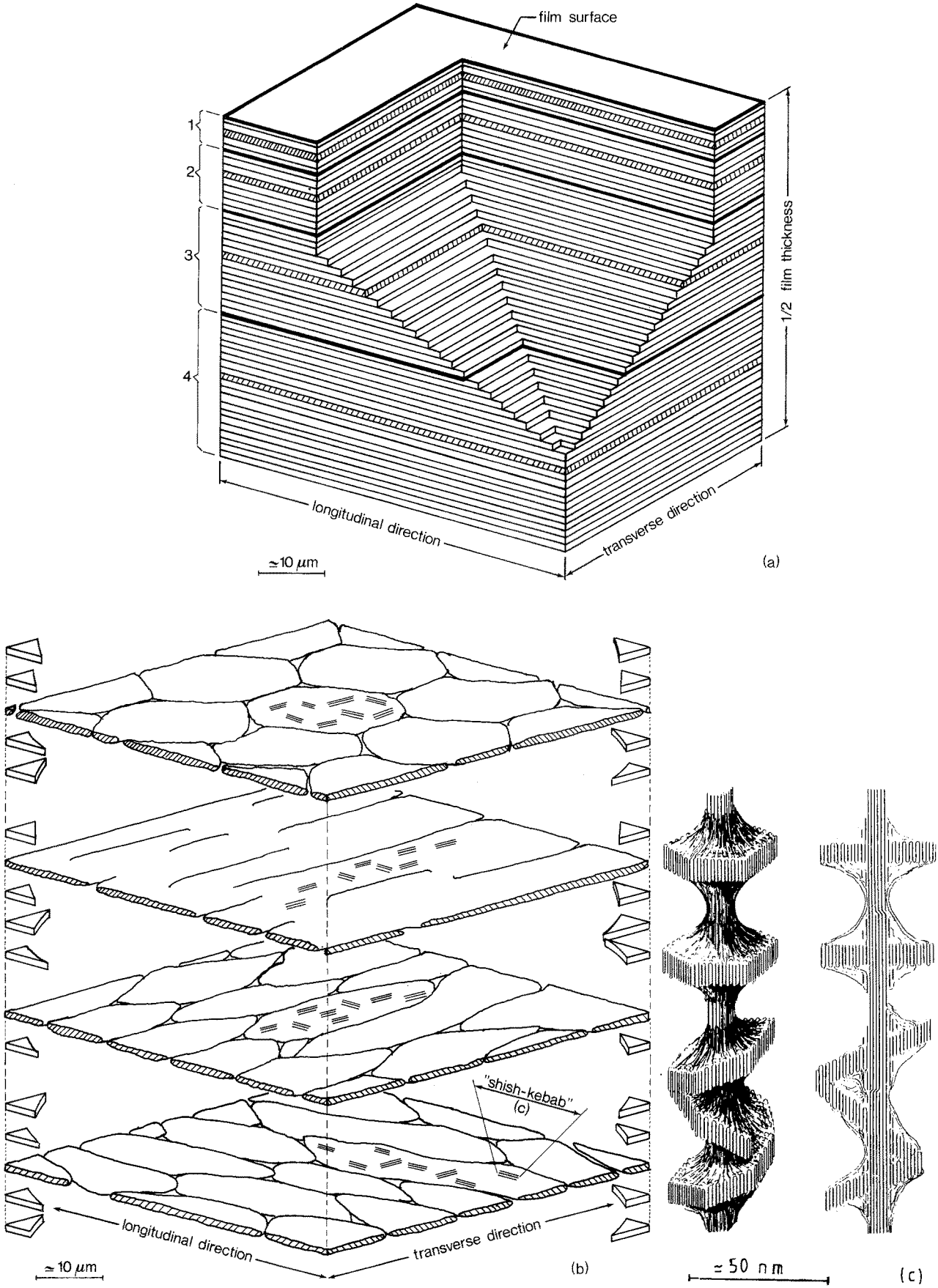

Figure 14 Structure of the biaxially stretched and thermofixed PET film. The laminated structure, parallel to the film surface [13]. The layers can be grouped into equally oriented stacks (four in this figure). The thinner the stacks are, the more laminated is that part of the film. Layers of unequally oriented stacks are shown separately [13]. Different crystal superstructures (i.e. the layer substructures) are schematically presented. (c) The most common extended crystal structure, namely the "shish-kebab", typical for crystallization under flow (from Pennings [6]).

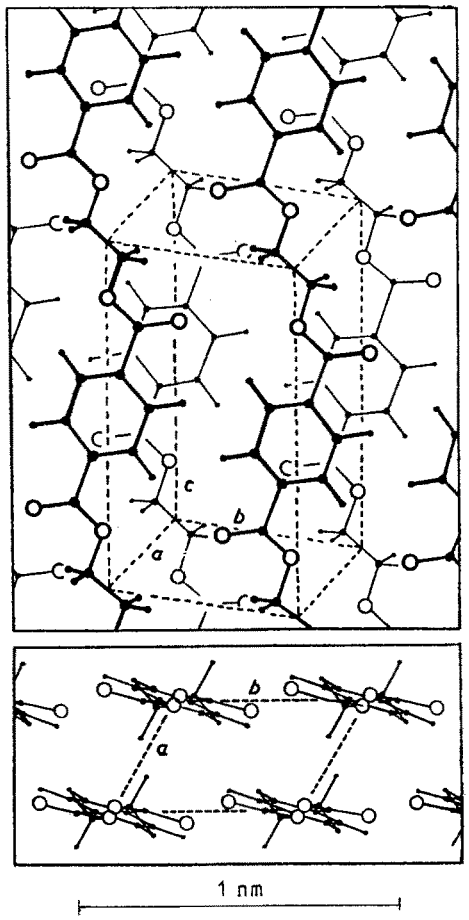

Figure 15 Unit cell of crystalline PET, with repeating unit -[CH_2-O-CO-C_6H_4-CO-O-CH_2-] along the *c*-axis. The phenyl rings almost coincide with the (1 0 0) plane. (From Daubeny *et al.* [7].)

plane by rotation about their axis, their dimension in transverse direction has grown, and their thickness decreased. In addition, local orientations in "stacked" layers may differ strongly from each other [12, 13]. Still fewer polymer chains remained in the perpendicular direction.

4.1.4. Microstructure after thermofixing

The film is thermofixed at a temperature above 200° C, increasing the crystallization degree from 25% to 50%. This is mainly due to a perfection and growth of the existing oriented crystallites and to a crystallization of oriented amorphous phase, because the orientation distribution does not substantially change. The film contains two groups of shish-kebab crystals, mostly oriented in the longitudinal and transverse directions. Only a small amount of amorphous phase remains, but stacking defects, crystal borders, etc., give rise to a lower crystallinity than expected. In addition, the laminated character of the film increases because more molecules choose to be part of an oriented structure. Fig. 14 [13] gives a schematic representation of the film structure. It has a great influence on the subsequent cutting.

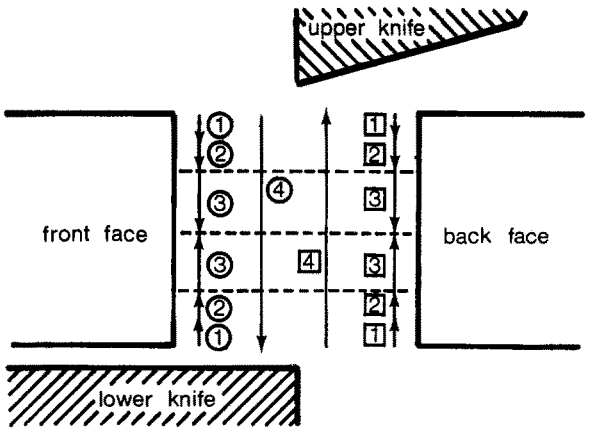

Figure 16 Schematic illustration of the four cutting phases (1, compressing phase; 2, shearing phase; 3, tearing phase; 4, damaging phase). At the left (numbers in circles), the actions of the knife edges on the front face are presented, and at the right (numbers in squares), the actions on the back face. Downward arrows show upper knife actions, upward arrows show longer knife actions.

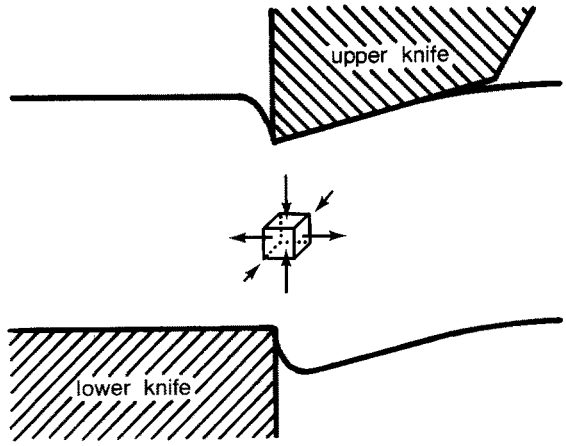

Figure 17 Normal stress components on an elementary volume particle in the middle of the film, during the compressing and shearing phases.

4.2. Description of the cutting process

A general description has been given previously [2, 14, 15]. Here, the cutting process will be described in a more appropriate and detailed way.

The cutting process can be divided into four phases (schematically presented in Fig. 16). Starting from both knife edges, one can successively discern the compressing phase, the shearing phase and the tearing phase. Shearing and tearing are responsible for the separation. The damaging phase (fourth phase) occurs from the beginning of the shearing phase at both faces, until total loss of contact between upper knife and front face, and between lower knife and back face. This happens at a later time than the moment at which the two knife edges touch each other.

4.2.1. Description of the compressing phase

Initially, the film is elastically compressed by the upper and lower knife, without forming a cut. A simplified stress analysis of this moment [2, 14, 15] gives the normal stress components on an elementary volume particle (Fig. 17): a compressive component perpendicular to the film; a small tensile component in the transverse direction, except at the knives, where the film is strongly compressed; a compressive component in the longitudinal direction. Of course, shear stresses play the most important role. A (simplified) qualitative Mohr's circle for the middle of the film is shown in Fig. 18a.

4.2.2. Description of the shearing phase

The film part lying under the upper knife is pushed to

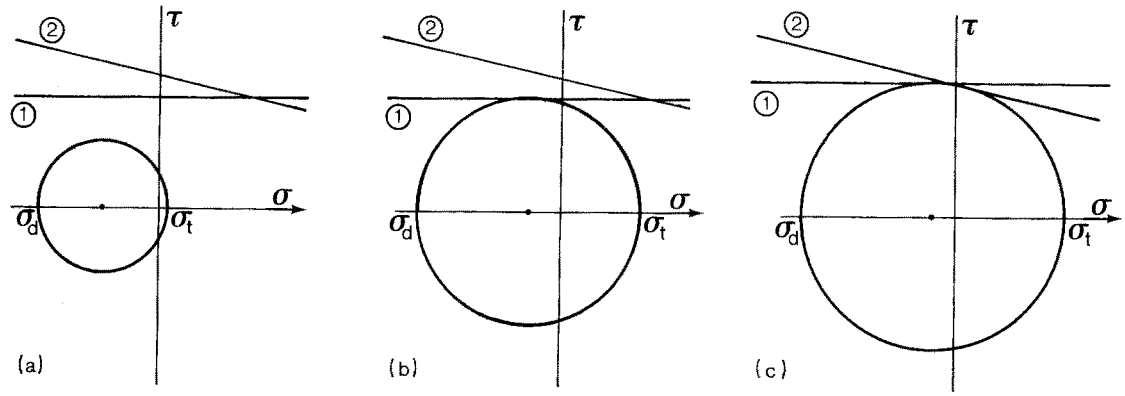

Figure 18 Simplified, qualitative Mohr's circle for the middle of the film, during the compressing phase (a), at the beginning of the shearing phase (b), and at the start of the tearing phase (c); σ_d is acting in the thickness direction, σ_t in transverse direction; line 1 is the shear yield locus, line 2 the shear tear locus.

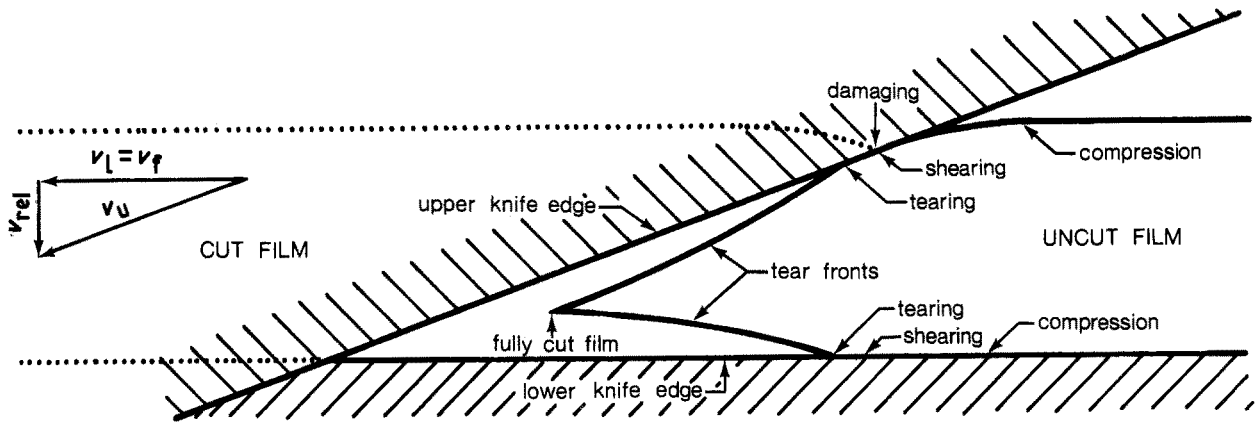

Figure 19 Schematic illustration of the formation of the front face, with the starting-points of the different cutting phases at the upper knife and the lower knife edges.

the right, whereas the left part is prevented by the upper knife from following this movement. Transverse tensile stresses grow to a greater extent than the compressive ones [2]. When the material reaches the shear yield locus (Fig. 18b), the knives penetrate into the film and a cut forms.

4.2.3. Description of the tearing phase

By strengthening the material, the stresses still increase. The shear tear locus, a descending straight line in the Mohr's diagram, will be reached (Fig. 18c). The film is now split by a tear, starting at the knife edges and following a path of minimum energy with only little plastic deformation.

Because the lower knife has a zero knife angle, stresses are growing more slowly and cutting starts somewhat later. Thus, there are two tears, meeting somewhere in the middle of the film. Fig. 19 shows (qualitatively) the different phases at the front face, starting from both knives. Initially, tearing speed is high, but decreases all the time, until the two tears meet each other. This is expressed in Fig. 19 by the particular routes of the tearing phase boundary lines, relative to the knife edges. The slope of the tears becomes almost parallel with the knife edges.

4.2.4. Description of the damaging phase

The sheared edges still lie beside the knives after separation (Fig. 3). Some parts are even not passed by the knife edges. As the knives penetrate further, they continue to damage the sheared edges, which also damage each other by friction.

4.3. Explanation of the sheared edges

4.3.1. Formation of the scales

Because PET is a rather tough material, it is highly compressed before it is cut (Figs 17 and 19). The cut front propagates step by step in the longitudinal direction, because it ends up in a less stressed zone, but especially because the film has no homogeneous microstructure. Indeed the propagation is retarded at resisting transverse oriented shish-kebab crystals.

The newly formed sheared edge is immediately damaged, e.g. at the front face by the upper knife, giving a flat surface with vertical tracks of the knife roughness. However, elastic energy was stored in the compressed material. When tearing starts, it is freed and the cut part jumps upwards (step by step in the longitudinal direction). It partly strikes against the descending upper knife and some pinched material is scraped off and spread over the edge (Fig. 20). This damaging effect forms scales that overlap the underlying surface. Similarly, scales are formed at the bottom of the back face by the lower knife action.

Because PET is a visco-elastic material, its toughness decreases with deformation rate. At low cutting speed, the film must be strongly compressed before it is cut. A lot of material is pinched, and long scales

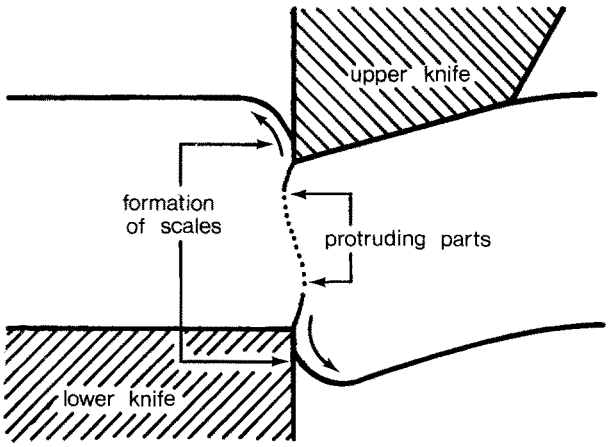

Figure 20 Upward movement of the front face (and downward movement of the back face) during separation, causing the formation of scales (part of the damaging phase). The profiles of the front face and the back face exhibit protruding parts, which are responsible for the formation of the split regions.

form. At higher speed, PET is more brittle, and short scales form. This results in a logarithmic relationship between the relative scale length and the initial compressive strain rate, as shown in Fig. 8.

The relative scale density decreases at higher speeds because the film is more brittle then and cut by relatively larger steps in the longitudinal direction.

4.3.2. Formation of the split region

The damaging phase forms scales and folded flaps, and also the split region. The front face, for example, has a profile as shown in Fig. 20, with a protruding part, formed by the cut of the lower knife. The descending upper knife (and PET material of the back face) "catch" (mostly by friction) the emerging part, which is compressed and horizontally split. This splitting is facilitated by the layered film structure. A similar situation takes place at the top of the back face by the lower knife (and front face material) action.

4.3.3. Formation of the flaps regions

The tear avoids breaking polymer chains as much as possible and can considerably change direction, as reported earlier by Friedrich for the fracture of spherulitic crystal structures [16]. *A fortiori*, the same can be said for oriented structures. For the longitudinal shish-kebab crystals, weak secondary van der Waals forces have to be broken. The tear easily separates (or divides) them, which forms the rugged, lamellar surface between the flaps. It requires a lot of energy, however, to break transverse shish-kebab crystals. Therefore, layers are sometimes surprisingly left intact. They are (at least partially) pulled out of the edge to form a flap at one edge and a hole at the other edge. The tear follows the path of minimum energy, although it is a much longer one. The more the film is layered, the easier are flaps formed. They can form at both edges.

The flaps have a slope as shown in Fig. 4 because they are formed by two different tears (Fig. 19). As the slope of the upper tear is positive at the front face, the upper flaps also have a positive slope. The slope of the lower flaps will be negative. At the back face, the same

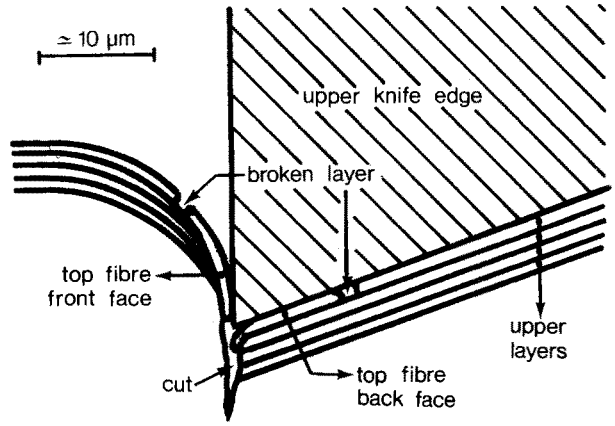

Figure 21 Formation of the top fibres at the front face and the back face, caused by the knife edge friction on the upper film layers.

occurs, but of course an opposite slope is seen in the photographs (see direction of crack propagation in Fig. 4).

At the front face, the flaps will be folded downwards and even fastened again by the descending motion of the upper knife (and PET material of the back face). Conversely, the flaps at the back face are spread upwards.

4.4. Explanation of the formation of fibres

4.4.1. Formation of the top fibre at the front face

This fibre is formed when the compressed, tearing film relaxes by tipping up. The upper layer of the film rubs against the upper knife with a high frictional force (Fig. 21). It possibly detaches from the underlying layers and breaks. A thin ribbon-like fibre is formed.

The formation is dependent on the cutting parameters. Because the film is less compressed before cutting at high speed (more brittle) and with thinner film, the frictional force is smaller and fewer fibres are formed. Smaller knife angles and a blunt upper knife increase the compression (and thus fibre formation) because they give rise to a lower stress concentration (shearing starts later).

Because of the upper knife angle, and because the film is supported by the lower knife, the back face does not contact the lower knife as forcefully as the front face contacts the upper knife. Therefore, this fibre is rarely formed at the bottom of the back face. The frictional force seems to be high enough to form scales, but not enough to detach the bottom layer.

4.4.2. Formation of the top fibre at the back face

This fibre (Fig.11) shows up at the same place as the previous one, but at the back face (Fig. 21). It is formed in a similar way but by a different frictional force. As the upper knife has a knife angle, it pushes the back face down to the right with a high compressive force. The accompanying frictional force can detach a part of the top layer of the back face to the left. The layer is stretched and breaks. A thin ribbon-like fibre is formed.

The top fibre at the back face forms with wider cutting angles, because there's a larger tangential displacement between upper knife and film. Secondly, a

thicker film demands higher forces over a lager displacement, stimulating the fibre formation. Finally, lower cutting speeds cause larger deformations, thus larger displacements, but smaller forces, and this results in more critical fibre formation.

This kind of fibre does not show up at the bottom of the front face because the lower knife has a zero knife angle (no tangential displacement), and because the film is supported by this knife during cutting. However, another fibre can show up there (see Section 4.4.3).

4.4.3. Formation of the bottom fibre at the front face

This fibre has been mysterious for a long time because it is not the only one that is found at the bottom of the front face. Other fibres are sometimes carried along to that point by the upper knife motion and even fastened again to the edge, giving rise to erroneous conclusions about their origin. However, a specific fibre (Fig. 12) forms during the formation of the split region at the front face when material is pulled loose by the friction which occurs (see Section 4.3.2). Low cutting speeds, a blunt lower knife and thick films give rise to a large protruding edge, which increases the chance of bottom fibres being produced.

Formation at the top of the back face seems to be less probable because the back face can move more freely.

4.4.4. Formation of the central fibre

The central fibre (Fig. 13) is formed in the flaps regions. If a knife (or opposite edge) cuts or rubs a flap, it can break, which results in a very thin fibre (Fig. 22). Because the contact between the upper knife and the front face is more forceful than between the lower knife and the back face, the fibre mostly forms at the front face. As already seen, more and larger flaps are present at higher speed, increasing the chance of fibre formation. However, the flaps are usually only spread over the edge without being broken or cut.

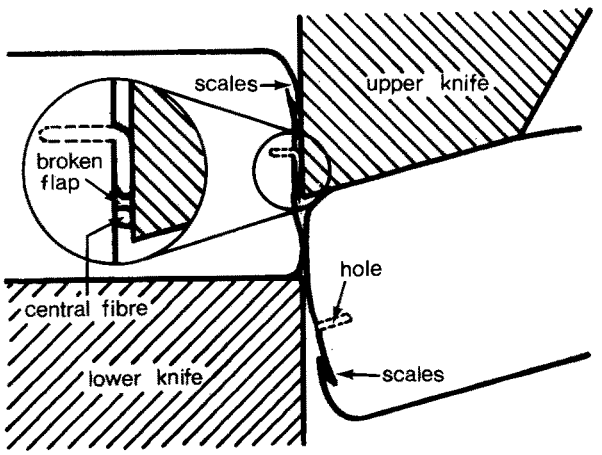

Figure 22 Formation of the central fibre at the front face. After a flap has been formed at the font face, its tip breaks by striking against the upper knife.

5. Conclusion

During the production of PET film, a laminated structure is obtained, with the chains mainly oriented in longitudinal and transverse directions. The subsequent cutting process can be divided into four phases: a compressing phase, a shearing phase, a tearing phase and finally a damaging phase.

The two edges of the cut film, namely the front face and the back face, can show four different regions: a scales region, an upper flaps region, a lower flaps region and a split region. They are closely related to the cutting phases and the PET microstructure, as well as to the cutting parameters i.e. cutting speed, knife angle and film thickness.

The same can be said of the fibre formation, which is a particular cutting defect. Three kinds of fibres are observed after shear cutting: a top fibre at the front face and the back face, a bottom fibre at the front face and a central fibre.

Acknowledgements

The authors thank ir. L. Tack for the information on stress conditions in the sheared zone, given in his final thesis. They also thank Drs I. Verpoest and L. Doxsee, Department of Metallurgy and Materials Engineering, Catholic University of Leuven, B3030 Heverlee, Belgium, for carefully reading and revising the manuscript.

References

1. M. B. BEVER (ed.), "Encyclopedia of Materials Science and Engineering" (Pergamon, New York, 1986).
2. M. FEILER, Doctoral Thesis, Technische Hochschule, Stuttgart (1970)
3. CIRP, in "Dictionary of Production Engineering 3 Sheet Metal Forming" (Girardet, Essen, Germany, 1965) nos. 2055, 2174.
4. N. J. MILLS, in "Plastics: Microstructure, Properties and Applications" (Edward Arnold, London, 1986) pp. 35, 122.
5. H. J. BIANGARDI and H. G. ZACHMANN, *J. Polym. Sci. Polym. Symp.* **58** (1977) 169.
6. A. J. PENNINGS, *ibid.* **59** (1977) 55.
7. R. de P. DAUBENY, C. W. BUNN and C. J. BROWN, *Proc. Roy. Soc. London* **226** (1954) 531.
8. K. MATSUMOTO, Y. IZUMI and R. IMAMURA, *Sen-I Gakkaishi* **28** (1972) 189.
9. M. TAKAYANAGI, K. IMADA and T. KAJIYAMA, *J. Polym. Sci.* **15** (1966) 427.
10. R. BONART and R. HOSEMANN, *Kolloid Z.* **186** (1962) 16.
11. K. MATSUMOTO, Y. IZUMI and R. IMAMURA, *Sen-I Gakkaishi* **28** (1972) 179.
12. K. MATSUMOTO, H. IEKI and R. IMAMURA, *ibid.* **27** (1971) 516.
13. J. DENEIR, unpublished results.
14. H. HOJO, *Ann. CIRP* **14** (1967) 409.
15. L. TACK, Thesis, Katholieke Universiteit, Leuven, 1986.
16. K. FRIEDRICH, in "Proceedings of the 4th International Conference on Fracture: Advances in Research on the Strength and Fracture of Materials 3B Applications and Non-Metals", Waterloo (Canada), June 1977, edited by D.M.R. Taplin (Pergamon, New York, 1978) p. 1119.

Received 7 March
and accepted 26 July 1988